Influence of Substituents on the Anharmonicity of ν_s(OH) Vibration in Phenol Derivatives Explored by Experimental and Theoretical Approach

Bogusława Czarnik-Matusewicz,* Maria Rospenk, Aleksander Koll, and Janez Mavri†

Faculty of Chemistry, University of Wrocław, 14 F. Joliot-Curie, 50-383 Wrocław, Poland, and National Institute of Chemistry, Hajdrihova 19, Sl-1001 Ljubljana, Slovenia

Received: October 1, 2004; In Final Form: December 20, 2004

Very good reproducibility of the first five vibrational transitions of phenol in the gas phase by the MP2/6-31G** potential for O−H bond stretching was found. The vibrational levels were calculated by a program for variational solving of the time-independent Schrödinger equation in one dimension. Relative intensities of particular transitions were determined on the basis of the function of the dipole moment. The substituent effects on the ν_s(OH) transitions and on the intensity of these transitions, as well as on the structure of eleven phenols, was analyzed as a function of the pK_a values.

1. Introduction

Phenols form with various bases very convenient model systems in the study of the nature of hydrogen bonding.[1] They are especially useful because of the very wide range of pK_a values available. One of the interesting features of these systems is the anharmonicity of the ν_s(OH) vibrations, which increases with the strength of interactions and is responsible for modification of the frequency and the intensity of the ν_s(OH) vibrations. It is known that these vibrations are also anharmonic in phenol itself,[2] as well as in its derivatives.[3,4]

The quantum mechanical calculations now are very widely applied to describe various properties of molecules, but it appears that the available programs of Gaussian or Gammes type, based on harmonic approximation, are not able to reproduce the anharmonicity in the free phenol derivatives or in their complexes.

There are a few recent papers on the properties and spectroscopic force field of phenol.[4−12] It was shown[5] that the DFT BLYP/6-31G** method only gives a 50-cm^{-1} higher frequency of the $0 \rightarrow 1$ transition in phenol than that measured in CCl_4 solution (3611 cm^{-1}). However, this level of theory leads to lower values of calculated frequencies than the experimental ones for more than 50% of transitions.[7] Other methods elevate ν_s(OH) frequency about 200 cm^{-1}. Several studies[4−10] demonstrate that quantum mechanical methods in harmonic approximation cannot reproduce the ν_s(OH) frequency even if one applies the frequency correlation factor, because the ν_s(OH) transitions are more anharmonic than other modes. Because of these reasons, the problem of proper description of anharmonicity in phenol-type molecules appears to be very important. It requires construction of a reliable potential, on the basis of which one can properly reproduce the frequencies of experimental transitions. The calculation of the potential surface is a challenging task, mainly for many-atoms systems. Such an approach, published recently, solves the problem by pointwise calculations of the potential energy surface used for the construction of a computationally inexpensive function followed by solving the vibrational Schrödinger equation. Calculations concerning systems composed from 15−21 atoms,[13] revealing strong coupling of the ν_s(OH) mode with low-frequency transitions,[14] were performed by using this method. A different approach to this problem has been proposed by Chaban et al.[15] and Del Bene and Jordan[16] where force constants were scaled. In tests, although on smaller systems, calculated anharmonic frequencies presented satisfactory agreement with the experimental data.

In this paper, we apply the one-dimensional numerical potentials resulting from the energy calculations at different OH distances with the aim of reproducing the anharmonic ν_s(OH) frequency and intensity in phenol and its derivatives. Both ours and the afore-mentioned calculations of the potential energy distribution (PED)[4−9] demonstrate clearly that the normal coordinate of ν_s(OH) vibration in phenol and its derivatives consists predominantly of the OH-bond length changes. With this method,[13] we are able to reproduce up to the 6th experimental vibrational energy levels of phenol using the one-dimensional proton potential function calculated by the MP2/6-31G** method. With the same procedure, we shall determine the potentials for 11 derivatives of phenol in order to correlate the experimentally determined frequencies and intensities of the fundamental transitions and the first two overtones with the calculated values. The structural parameters are also related to the electronic interaction between the substituent and the reaction center (the OH group in our case). We are going to correlate the spectroscopic and structural consequences of such interactions, obtained on the basis of the most reliable theoretical methods, with the pK_a values of phenols.

2. Methods

2.1. Experimental Section. The following 11 phenols have been the subjects of the studies presented: 3,5-dichlorophenol (35DClPh), 3,4-dichlorophenol (34DClPh), 3-bromophenol (3BrPh), 4-bromophenol (4BrPh), 4-chlorophenol (4ClPh), phenol (Ph), 4-methylphenol (4MPh), 2,5-dimethylphenol (25DMPh), 2,3-dimethylphenol (23DMPh), 2,6-dimethylphenol (26DMPh), and 2,4,6-trimethylphenol (246TMPh). All the compounds and carbon tetrachloride were commercially available from Aldrich. Phenols were crystallized from a petroleum

* Corresponding author: bc@wchuwr.chem.uni.wroc.pl.
† National Institute of Chemistry.

10.1021/jp0455273 CCC: $30.25
Published on Web 02/18/2005

TABLE 1: Calculated and Experimental Characteristics of the Anharmonic ν_s(OH) Oscillator in the Phenol Molecule

method	BLYP/ 6-31G**	B3LYP/ 6-31G**	B3LYP/ 6-311++G**	MP2/ 6-31G**	exp. 19
		Eigenvalues (E_n) (kcal/mol)			
E_0	5.050	5.268	5.300	5.359	
E_1	14.780	15.462	15.547	15.709	
E_2	24.345	25.198	25.306	25.592	
E_3	32.838	34.467	34.611	35.005	
E_4	41.271	43.302	43.447	43.964	
E_5	49.727	51.897	52.005	52.652	
		Transitions (E_n-E_0) (cm^{-1})			
$0 \rightarrow 1$	3411.3	3575.0	3593.4	3629.0	3656
$0 \rightarrow 2$	6657.9	6989.3	7015.7	7095.4	7143
$0 \rightarrow 3$	9745.3	10239.9	10278.9	10396.8	10461
$0 \rightarrow 4$	12702.4	13338.2	13377.3	13538.5	13612
$0 \rightarrow 5$	15668.0	16352.4	16379.0	16585.4	16590
calculated harmonic frequency (cm^{-1})[a]	3661	3826	3839	3878	
anharmonicity constant X (cm^{-1})[b]	−70.9	−76.9	−79.9	−78.7	−84.5
fitted harmonic frequency ω_e (cm^{-1})[b]	3543	3725	3749	3784	3825
equilibrium OH distance R_e (Å)[a]	0.9775	0.9661	0.9628	0.9655	
OH distance at $n = 0$ R_0 (Å)	0.9846	0.9722	0.9687	0.9713	

[a] Direct output from *Gaussian 98*. [b] Obtained from eq 1.

ether mixture, either sublimated or distillated. The solvent was dried on molecular sieves.

Both the mid-infrared (MIR) and near-infrared (NIR) spectra of these phenols in carbon tetrachloride solution, at a concentration of 0.05 mol/dm^3, were measured on a Bruker 66 and a Nicolet Magna 760 spectrometer at room temperature. The following instrumental parameters were selected for the MIR measurements: KBr beam splitter, Globar source, and DTGS detector. The spectra were collected at 1-cm^{-1} resolution by using KBr cells with path lengths selected from the 0.1−0.2-mm range. During the NIR measurements, different detectors were used on the two instruments (Bruker, cooled InSb; Nicolet, cooled MCT/A), whereas all other parameters were the same i.e., CaF_2 beam splitter, tungsten source, 1-cm^{-1} resolution, and quartz-infrasil cells with path lengths of 5 and 10 cm. Data processing was aimed mainly at removing a fluctuating baseline and noise; also, the evaluation of parameters of the ν_s(OH) bands in a range of a fundamental, a first, and a second overtone transition was performed by the Grams 32/AI software (Galactic Ind. Corp.). To make sure that the observed differences in band parameters are free of any instrumental artifacts, some selected samples were measured on the two spectrometers in the same spectral region. Moreover, the measurements in the range of the second overtone were repeated at least three times for separately prepared solutions of very similar concentrations.

2.2. Theoretical Section. The vibrational time-independent Schrödinger equation for the OH coordinate was solved numerically using the two-boundary-conditions approach. It is based on the Numerov algorithm and is described in detail in ref 13. A related variational-theory-based program package is described in ref 17. Both programs can be obtained free of charge from one of the authors (J.M.). The first step of the method comprises calculations of potential energy at 20 different fixed values of O−H coordinates within the range 0.8−2 Å by using the *Gaussian 98* v. A.11.1 program.[18] Calculations for phenol were carried out at the BLYP and B3LYP density functionals with two different basis sets, 6-31G** and 6-31++G**. MP2 computations were done only with the 6-31G** basis set. For 10 derivatives of phenol, the B3LYP and MP2 methods with the 6-31G** basis set were chosen. In the next step, the pointwise surfaces were fitted to a form suitable for solving the one-dimensional Schrödinger equation. Finally after solving the equation, the eigenvalues (energies) and eigenfunctions (wave functions) of the first 6 vibrational levels were directly obtained. Furthermore, on the basis of the values of dipole moments for particular OH distances, the intensities for the first few transitions have been calculated.

3. Results and Discussion

3.1. Anharmonicity of the O−H Stretching Vibrations in Phenol. According to the description giving in the preceding section, the anharmonic ν_s(OH) frequency and intensity of phenol were determined using the numerical, one-dimensional potential for stretching of the O−H bond. However, before such data are utilized, the calculation procedure should be verified. It can be done in a test where computed transitions are compared with the experimental ones. Such experimental information is not common in the literature, but fortunately, the five lowest levels for the ν_s(OH) vibrations of phenol in the gas phase were determined in supersonic jet conditions.[19] These very low temperature measurements allow the avoidance of the complications arising from hot transitions. For the properly constructed potential, at least a few of the lowest experimental vibrational levels should be reproduced. Moreover, the gas-phase results[19] are especially suitable for comparisons of the ab initio and DFT data calculated with different basis sets. Thus, calculations for the phenol were carried out at four different levels. A comparison of the numerical eigenvalues with measured frequencies will let us test various quantum-chemical levels of theory in the calculations of vibrational levels of the anharmonic potential. It is a well-documented fact that calculated values of different molecular properties strongly depend on the quality of the basis set and the extent of electron correlation.[16,20]

The results of calculations together with the experimental values are shown in Table 1. The value of the harmonic frequency (ω_e) and the anharmonicity constant (X) were obtained from a fit of the energy of transitions (i.e., the differences between successive eigenvalues E_n and E_0) to the two-parameter expression

$$\nu^{0n}/n = (E_n - E_0)/n = nX + (\omega_e + X) \qquad (1)$$

determined from following formula

$$E_n = \omega_e(n + {}^1/_2) + X(n + {}^1/_2)^2 \qquad (2)$$

that describes energy of the nth vibrational level in a frame of

TABLE 2: Vibrational Matrix Elements, R_{ij} (debye), Calculated for ν_s(OH) and ν_s(OD) Stretching Vibrations in the Phenol Molecule

Phenol (OH)	
$R_{01} = +0.067313 \cdot 0.711 + 0.002306 \cdot 0.17 + 0.001008 \cdot (-1.266)$	
$R_{02} = -0.007456 \cdot 0.711 + 0.006070 \cdot 0.17 + 0.000416 \cdot (-1.266)$	
$R_{03} = +0.001370 \cdot 0.711 - 0.001595 \cdot 0.17 + 0.000597 \cdot (-1.266)$	
$R_{01} = +0.047850 + 0.000392 - 0.001276 = +0.046975$	$(R_{01})^2 = 2.21\ 10^{-3}$
$R_{02} = -0.005300 + 0.001032 - 0.000527 = -0.004796$	$(R_{02})^2 = 2.30\ 10^{-5}$
$R_{03} = +0.000974 - 0.000271 - 0.000756 = -0.000053$	$(R_{03})^2 = 2.81\ 10^{-9}$
Phenol (OD)	
$R_{01} = +0.056398 \cdot 0.711 + 0.001057 \cdot 0.17 + 0.000567 \cdot (-1.266)$	
$R_{02} = -0.005301 \cdot 0.711 + 0.004360 \cdot 0.17 + 0.000172 \cdot (-1.266)$	
$R_{03} = +0.000828 \cdot 0.711 - 0.000994 \cdot 0.17 + 0.000385 \cdot (-1.266)$	
$R_{01} = +0.040099 + 0.000180 - 0.000718 = +0.039561$	$(R_{01})^2 = 1.56\ 10^{-3}$
$R_{02} = -0.003780 + 0.000741 - 0.000218 = -0.003257$	$(R_{02})^2 = 1.06\ 10^{-5}$
$R_{03} = +0.000589 - 0.000169 - 0.000487 = -0.000067$	$(R_{03})^2 = 4.49\ 10^{-9}$

the second-order perturbation theory.[21] Table 1 shows that among the tested methods the BLYP/6-31G** potential is much less suitable for calculations of the energy of transitions. The frequencies calculated from this anharmonic potential are ~200 cm^{-1} lower than the experimental frequencies. The anharmonic potentials obtained by the B3LYP/6-31G** and B3LYP/6-311+G** methods present substantial improvement in the calculations. However, the potential constructed on the MP2/6-31G** method appears to be the best for reproducing the experimental frequencies. Underestimation of the experimental values by calculations, expressed simply as $\Delta\nu^{0n} = \nu^{0n}_{exp} - \nu^{0n}_{MP2}$, is the smallest for the MP2/6-31G** method. The difference for the $0 \rightarrow 1$ transition has a value of 27 cm^{-1} and successively increases up to the $0 \rightarrow 4$ transition ($\Delta\nu^{04} = 74$ cm^{-1}), whereas for the $0 \rightarrow 5$ transition, it drops to 5 cm^{-1}. It is worth mentioning that such a small difference between experimental and theoretical data for the $0 \rightarrow 1$ transition has not been achieved in any earlier ab initio calculations for phenol.[4−10] A comparison of the results obtained with the B3LYP functional and different basis sets shows that the 6-31G** results are not seriously worse than the much more time-consuming calculations with the extended basis set 6-311++G**. Because the MP2/6-31G** potential faithfully reproduces the experimental energy levels for phenol in the best way, the MP2/6-31G** method has been selected to perform the calculations of the 10 various derivatives of phenol.

Similar conclusions that BLYP results underestimate both the harmonic and anharmonic frequencies and that B3LYP and MP2 methods give results of comparable quality were obtained in the calculation of the anharmonic vibrational states[22] by means of the other approach.[15] It can be expected that reparametrization of the B3LYP functional should improve the results, as it was obtained in calculations at the harmonic level.[23]

The calculated potentials also allow the determination of the equilibrium length of the O−H bond. The r(OH) values taken at the minimum of obtained potentials are higher than the value given in an electron diffraction experiment[24] (0.956 Å) and that directly extracted from Gaussian output; see Table 1. The differences indicate that further study of this problem is necessary, perhaps also from the experimental point of view. Nevertheless, the differences are within the limits of experimental uncertainty.

As was mentioned in the computational section, for each calculated vibrational level (E_n) its own eigenfunction (φ_n) was obtained that can be used for computation of other quantities. Among them, the most important for us are IR transition intensities. Anharmonicity of the ν_s(OH) vibration, examined primarily by the relation between frequencies of the fundamental and the overtone transitions, can also be monitored through analysis of their intensities. Unfortunately, the experimental intensities even for the few first overtones are rare. Therefore, there is special interest in approaches that are able to predict the vibrational intensities.[25−28] To solve the problem by a theoretical method, the vibrational wave functions and the dipole-moment function of the molecule have to be known. The wave functions obtained for anharmonic levels allow the examination of an effect of the mechanical anharmonicity on the intensity of subsequent transitions, while knowledge of the function that describes the dipole moment versus bond displacement allows the analysis of spectral consequences of the electrical anharmonicity. The two types of anharmonicity together contribute to the intensity of overtones, however not simply additive. It was found that for an isolated C−H chromophore mechanical anharmonicity is more important than electrical anharmonicity, especially for the intensity of higher overtones.[26] The quantities that contribute to the two types of anharmonicity have been also determined by the software[17] used for the calculation of the anharmonic potentials. For the intensity computations, the vibrational matrix elements, R_{ij}, of the ν_s(OH) vibrational transitions according to the general formulation have to be determined.

$$R_{ij} = \int \varphi_i \mu(r) \varphi_j \, dr \tag{3}$$

To perform the comparison with numerous works discussing the role of particular derivatives of the dipole moment in the intensity of the main transition and overtones, one can expand the dipole moment function into a series going thus beyond the electrical harmonicity approximation

$$\mu = \mu_{r_e} + \left(\frac{\partial \mu}{\partial q}\right)_{r_e} \cdot q + \left(\frac{\partial^2 \mu}{\partial q^2}\right)_{r_e} \cdot q^2 + \left(\frac{\partial^3 \mu}{\partial q^3}\right)_{r_e} \cdot q^3 + ... \tag{4}$$

and obtain the expression for the vibrational matrix element of an ij transition

$$R_{ij} = \left(\frac{\partial \mu}{\partial q}\right)_{r_e} \cdot \int \varphi_i q \varphi_j \, dq + \left(\frac{\partial^2 \mu}{\partial q^2}\right)_{r_e} \cdot \int \varphi_i q^2 \varphi_j \, dq + \left(\frac{\partial^3 \mu}{\partial q^3}\right)_{r_e} \cdot \int \varphi_i q^3 \varphi_j \, dq + ... \tag{5}$$

where $q = r(\mathrm{OH}) - r_e(\mathrm{OH})$.

The program gives the possibility of automatic calculations of the vibrational matrix elements for deuterium-substituted (OD) molecules. The results of such calculations for the two isotopomers are given in Table 2.

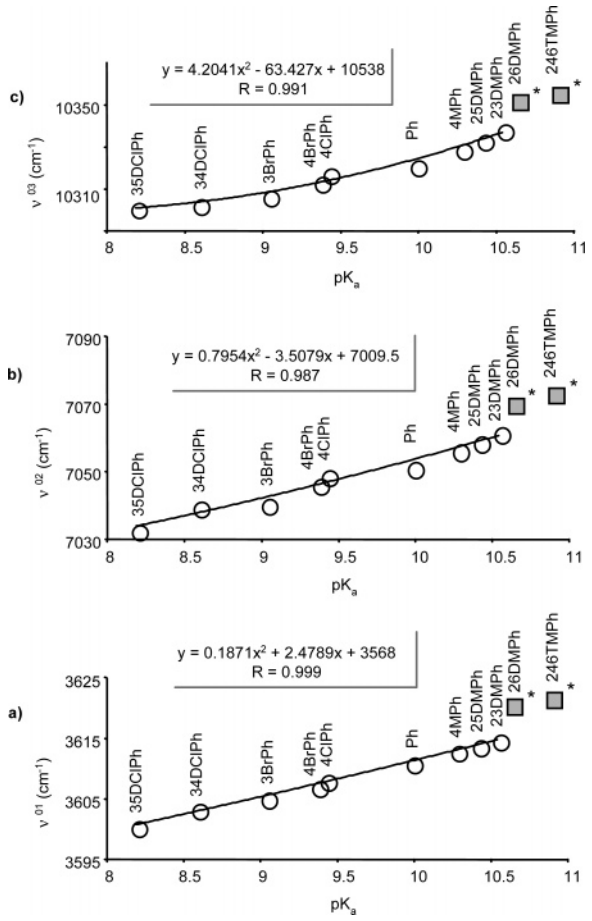

Figure 1. Positions of experimental band maxima of the fundamental (a), the first (b), and the second (c) overtone of ν_s(OH) transitions vs pK_a (data marked by * were excluded from correlation).

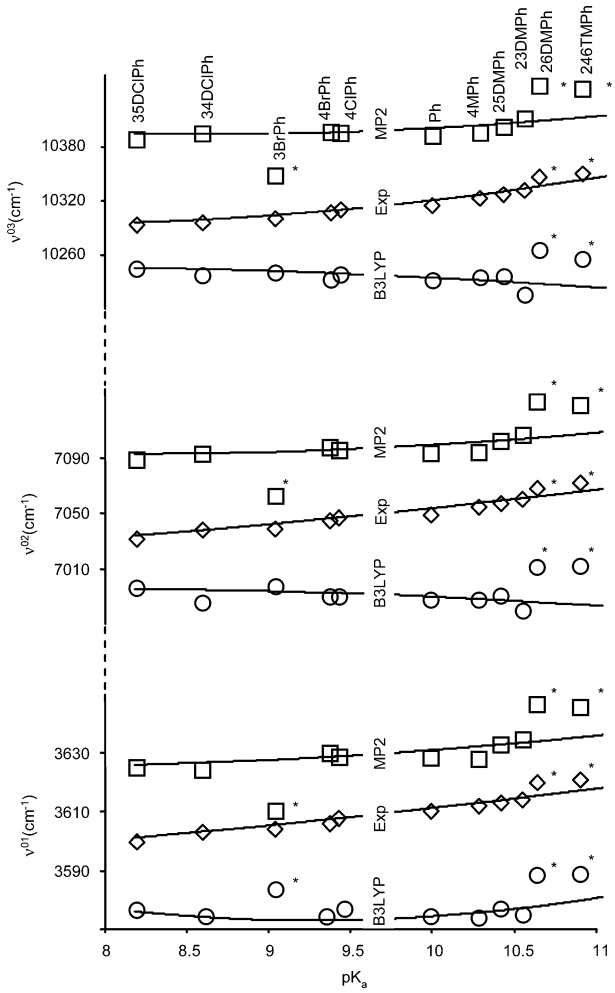

Figure 2. Positions of experimental and calculated band maxima of the fundamental and the first two overtones of ν_s(OH) transitions vs pK_a (data marked by * were excluded from correlation).

It is important to notice that the particular components of matrix elements for the first and higher overtones have different signs (while for the $0 \rightarrow 1$ transition, all the signs are the same) that causes a drastic falloff of intensity with increasing overtone level. For the effect, the decreasing values of particular parts of the integrals are also responsible. Comparison of the intensity for the two isotopomers shows that, similarly to the experimental data,[3b] the main transition and the first overtone for the ν_s(OD) vibration are less intensive than their OH counterpart. Analysis of Table 2 reveals that the differences arise from smaller values of the components correlated with the mechanical anharmonicity. Our earlier results from MIR−NIR measurements for phenol-OH and phenol-OD in CCl_4 point out on a similar relationship as the parameter X has 84.5 and 45.7 cm^{-1}, respectively.[3b] More experimental materials concerning the intensity of higher overtones measured for both isotopomers in the gas phase are necessary to verify the applicability of the presented approach to reproduce intensities of higher overtones.

3.2. Substituent Effect on Anharmonicity and the Structure of Phenol Derivatives. From the FT-IR spectra of 11 derivatives of phenol measured in the range of the main transition and the first two overtones in CCl_4 solutions, the band positions (ν_s^{0n}) and their intensities (Int^{0n}) were determined. Figure 1 presents the relation between the parameters ν_s^{0n} for the first 3 transitions and the pK_a values measured in aqueous solution at 25 °C.[29] The numerical pK_a values and the ν_s^{0n} values are listed in Table 1S (Supporting Information). The plots in Figure 1 show that for each transition there exists a precise ($R \approx 0.99$) curvilinear correlation between the ν_s^{0n} and pK_a parameters. Moreover, it also reveals that because of the mechanical anharmonicity for transitions characterized by a higher order of excitation the curvatures become larger. Only 2 points for each series are located outside the correlation. For the 2 phenols, steric repulsion between the methyl groups in the ortho positions and the OH group gives a larger frequency increase than can be expected from the obtained correlation. Acceptable correlation of the experimental OH-stretching frequencies with the aqueous pK_a values reveals that the spectral properties and acidity of these phenols depend on an effect of common origin. A similar conclusion has been obtained by Han et al.[12] where the parameters of the molecular structures of a series of 19 chlorophenols were correlated with the aqueous pK_a values.

For each of analyzed phenols, the numeric potentials for the O−H bond undergoing stretching vibration were calculated, and anharmonic ν_s^{0n}(OH) frequencies were determined at the MP2/6-31G** and B3LYP/6-31G** levels (Table 2S and 3S, respectively, in Supporting Information). Correlations between the pK_a parameters and the ν_s^{0n}(OH) values obtained from experiment and calculations are compared in Figure 2. As one can see for all three transitions, the MP2 calculations (for the gas phase) give values higher than the experimental ones (in CCl_4 solutions) that are higher than the B3LYP results. Figure 2 shows that the slope of the dependence on pK_a is reproduced much better by MP2 than B3LYP calculations. The points which

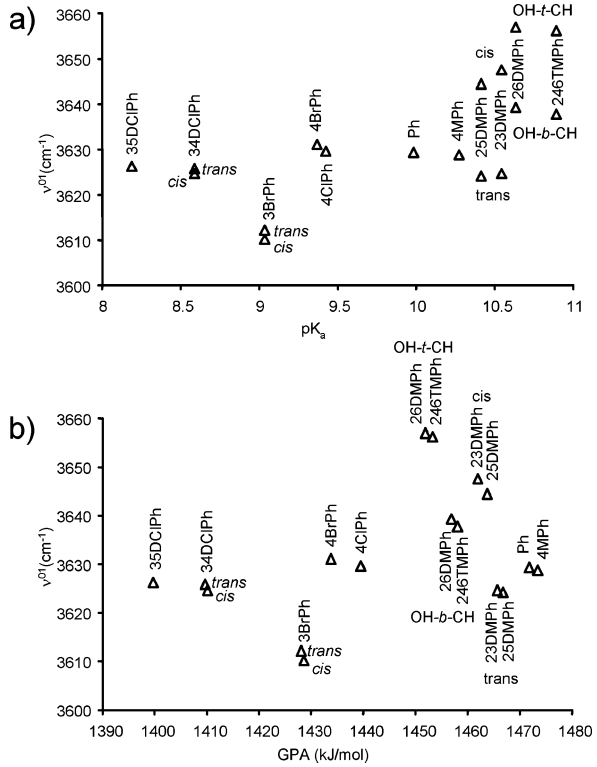

Figure 3. MP2/6-31G** calculated ν_s^{01} transitions for different OH conformers, plotted vs the pK_a (a) and GPA (kJ/mol) (b) values.

belong to 2,6-dimethyl derivatives have the same discrepancies from the correlations as was observed for experimental data.

Figure 3a shows the computed ν_s^{01} frequencies correlated with the pK_a parameters when different possible conformers have been accounted for in the MP2 calculations. For all asymmetric phenols, with substituents at meta and ortho positions, different energy minima for cis and for trans conformations appear. A detailed analysis of the influence of the halogen position on the features of the ν_s(OH) fundamental vibration has been given elsewhere.[4,12] The slightly lower ν_s^{01} values for cis than for trans halogenated conformers result from a weak attraction between O−H and Cl or Br atoms. Additionally, two notable configurations have been found for 2,6-dimethyl derivatives related to different conformations of the *o*-CH_3 group. In the OH-*t*-CH configuration, there is direct H···H contact between hydrogen atoms from the *o*-methyl and hydroxyl groups (see Scheme 1), whereas in the OH-*b*-CH structure, the H(OH) atom is positioned between two H(CH_3) atoms. For the two configurations, different electrostatic repulsion exists between the H(OH) and H(CH_3) atoms. For OH-*t*-CH, the repulsion is larger than for OH-*b*-CH, and thus, the frequency of the ν_s(OH) mode for the first structure is almost 20 cm^{-1} higher than for the second one. A very similar effect was found for the compounds with mono-*o*-methyl groups where cis conformers also give bands shifted ca. 20 cm^{-1} to higher frequencies. For the cis form, the OH-*b*-CH and OH-*t*-CH configurations were considered, and in Figure 3a, only the average value is given, similar to Figure 2. They were calculated according to the Boltzmann distribution at a room temperature. Recently, the splitting of the frequency of the ν_s(OH) mode due to the conformational isomerism was analyzed in detail both for phenols[4,30] and for alcohols.[31] Comparison of the calculated values with the experimental ones reveals that in real systems "average spectra" over different conformers are measured. Further analysis of the ν_s(OH) overtones where because of anharmonicity the differences between the conformers are larger has been undertaken, and results will be published.

SCHEME 1: Two Conformations of the OH Group in 2,4,6-Trimethylphenol

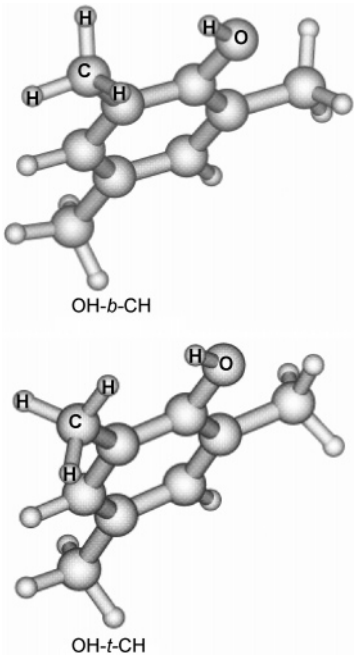

One can also mention that the theoretical values for the 3-Br derivative are remarkably separate from the correlation lines. A possible explanation is an inadequate quantum chemical description of the Br atom; a larger basis set should improve it. Generally, the experimental ν_s(OH) and that calculated at the MP2 level show a strong tendency to increase with pK_a. For the more-electron-donating substituent, both the measured and calculated ν_s(OH) frequencies are higher. Similar conclusions have been given elsewhere.[4,30] B3LYP calculations predict the tendency (Figure 2) that is in contradiction with the experiment.

The character of the correlation between the calculated vibrational frequencies and the pK_a values to a great extent depends on the fact that the two quantities relate to different media. The pK_a values are measured in aqueous solutions and reflect properties of the whole system with the interaction between phenols and water molecules, whereas the calculated vibrational frequencies relate to the gas phase and express intrinsic properties of the isolated molecules. Therefore, instead of the pK_a parameters, the intrinsic acidities of the phenols for the gas phase seem to be more appropriate in such a correlation.

The intrinsic gas-phase acidity (GPA), defined as the standard Gibbs' free-energy changes, GPA = ΔG^0_{acid}(PH)[32] for the reaction PH═P$^-$ + H$^+$, has been evaluated from energies of the neutral phenols (PH) and corresponding phenoxide ions (P$^-$) calculated at the MP2/6-31G** level of theory. Figure 3b presents the correlation between the vibrational frequencies and GPA parameters calculated for different possible OH conformers. Generally, the correlation between two intrinsic parameters (Figure 3b) is of a similar trend and quality as that between ν_s^{01} and pK_a parameters (Figure 3a). Figure 3b confirms the well-documented fact[30] that the ν_s^{01} bands of more acidic phenols have a larger red-shift effect. A more detailed analysis of Figure 3b allows us to state that the gas-phase calculated frequency depends on the contacts between O−H and C−H groups.

The O−H groups in ortho methyl derivatives, being in close proximity to the C−H groups, vibrate within the potential built of the intrinsic OH-bond stretching energy as well as the

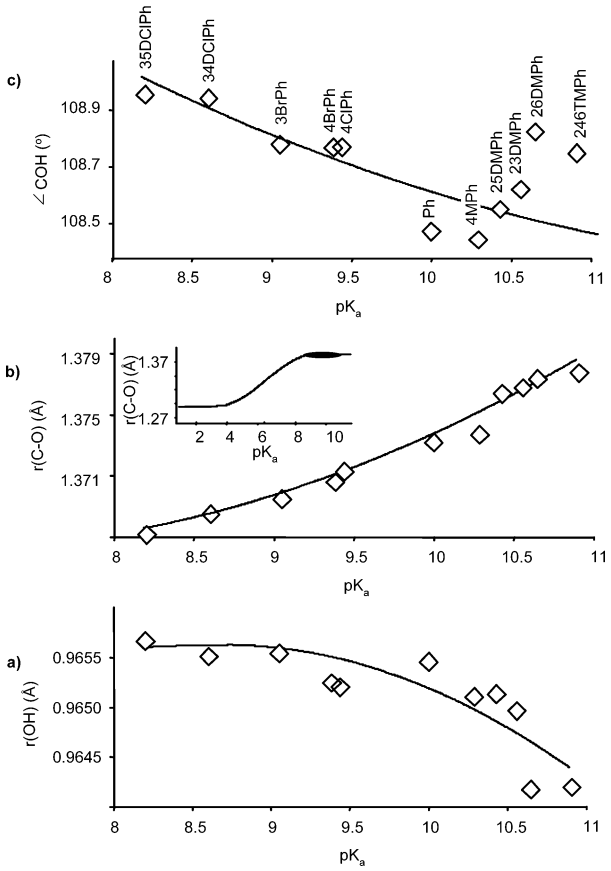

Figure 4. The structural parameters of phenols in functions of pK_a.

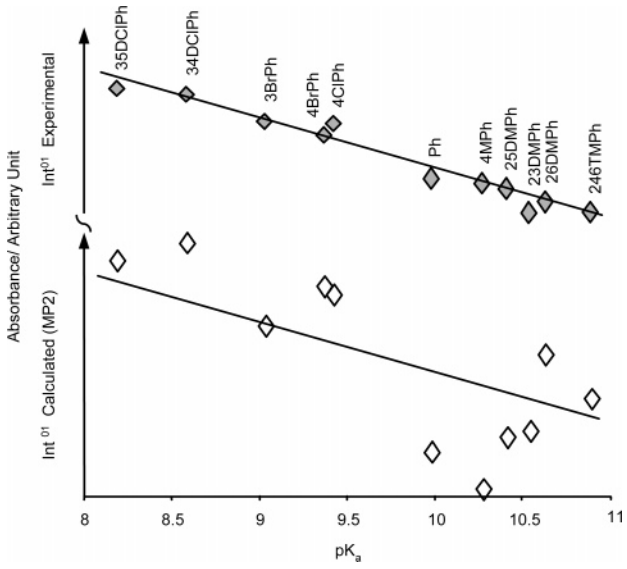

Figure 5. MP2/6-31G** calculated and experimental intensity of the $0 \rightarrow 1$ transition.

nonbonded interaction with the CH group that depends strongly on conformation of the methyl group (cf., for example, Scheme 1). On the other hand, the gas-phase acidity is related to phenolate energy, where the contacts between the O−H and C−H groups do not exist any more. Therefore, the calculated ν_s^{01} frequencies do not correlate better with the GPA than with the pK_a values. The exact numerical GPA values are given in Table 4S (Supporting Information). The obtained results reveal that whenever the acidity of phenols in the gas phase is controlled by steric and inductive effects, which are partially included in the GPA values, neither the GPA nor the pK_a parameters can be straightforwardly correlated with vibrational frequencies of the OH groups.

Figure 4 shows the structural changes (from MP2/6-31G** calculations) in phenols resulting from the electronic influence of substituents. The points for 2,6-dimethyl derivatives, where steric effects are also important, show more pronounced deviations from the correlations. One can mention the opposite effects of the substituents on the C−O and OH bond lengths. The substituents' withdrawing electrons increase the OH bond length and the COH angle, but decrease the C−O bond length. The electrons' withdrawal from a ring increases the C−O bond strength and weakens the OH bond, which was manifested by the shifts of the ν_s(OH) bands to lower frequency (Figures 1 and 2).

The observed trends are similar for the spectroscopic and structural effects of the increasing strength of hydrogen bonds. However, if one compares, for example, the correlation of r(C−O) on pK_a with changes of the C−O distance in phenol forming hydrogen bonds[33] (the pK_a scale in this part of Figure 4 is arbitrary), it appears that all the observed consequences of the substituents' influence are within the range characteristic for weak hydrogen bonds.

It was interesting to which extent the proposed model of intensity calculations is able to reproduce the experiment. One of the possible verifications is to compare the relative intensity of the $0 \rightarrow 2$ to $0 \rightarrow 1$ transition as well the $0 \rightarrow 3$ to $0 \rightarrow 1$ transition obtained in the experiment and by calculations. The verification will be done using average values of the intensity for all the 11 compounds studied.

Calculations give $\mathrm{Int}^{0\rightarrow2}/\mathrm{Int}^{0\rightarrow1} = 1.69 \cdot 10^{-2} \pm 1.42 \cdot 10^{-3}$ and $\mathrm{Int}^{0\rightarrow3}/\mathrm{Int}^{0\rightarrow1} = 6.22 \cdot 10^{-4} \pm 4.6 \cdot 10^{-6}$. The corresponding experimental values are $3.73 \cdot 10^{-2} \pm 7.7 \cdot 10^{-4}$ and $1.88 \cdot 10^{-3} \pm 1.66 \cdot 10^{-6}$ for the $0 \rightarrow 1/0 \rightarrow 2$ and $0 \rightarrow 1/0 \rightarrow 3$ transitions, respectively. It is seen that the calculations properly describe the order of intensity changes. The intensity of the $0 \rightarrow 2$ transition is $\sim 10^2$ times weaker than the fundamental ones, while for the $0 \rightarrow 3$ transition, it is about 10^3 times weaker.

The experimental values are about two times larger than the calculated ones. One has also to consider that the calculations were performed for the free molecules, while the experimental values were obtained in CCl_4 solutions where some increase of the intensity is due to polarization of CCl_4 molecules. The difference could also arise from the fact that in the applied approach the intramolecular couplings of the ν_s(OH) mode are neglected. Recently, it was shown that in a real system the OH-stretching vibration relaxes through the "doorway states" composed of the CH-stretching[10] and OH-bending[34] vibrations that significantly enhance intensity of the ν_s(OH) mode.

The experiment shows a decrease of the intensity of the $0 \rightarrow 1$ transition with growing pK_a (see Figure 5). The results of calculations present a similar correlation with pK_a. However, the spread of the results is much larger than in the experiment. It is well-known that the calculated dipole moment is a very sensitive quantity with respect to the applied quantum-chemical level of theory.[35] The calculated derivatives of dipole moments depend not only on a charge flow but also on many specific features of the particular substituents. With respect to experimental correlations, one can mention some kind of smoothing due to hydrogen-bonding interactions with CCl_4 molecules, which is proportional to the acidity of the OH groups, and therefore to pK_a values (see also ref 30).

The dispersion of the intensity values could suggest that there are essential differences in the shapes of the potentials and dipole-moment functions for these phenols. Therefore, the

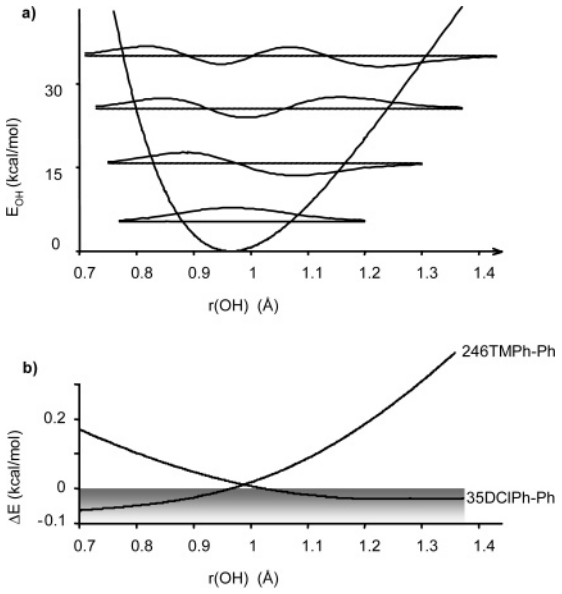

Figure 6. MP2/6-31G** potential curve and wave functions along the *r*(OH) distance for phenol (a) together with potential differences for selected phenols (b).

calculated potential for each derivative was compared with the one obtained for phenol together with the calculated eigenfunctions shown in Figure 6a. Comparison of the two phenols having substituents of very different properties is shown in Figure 6b. For 35DClPh, the electron-withdrawing substituents cause the potential to become steeper on the side of low *r*(OH) and shallower on the side of large *r*(OH) values, whereas the electron-donating methyl groups act in a reverse manner. The numerical results support a hypothesis that the increase of the slope of the inner wall leads to an increase of the intensity. While changes observed for 246TMPh reveal that for less intensive bands in this compound the potential becomes more harmonic (i.e., the slope of the inner wall decreases and of the outer increases). A similar conclusion that the intensity is extremely sensitive to small changes in the potential energy function has been obtained by Lehmann and Smith.[26] Moreover, they demonstrated the exponential decrease of the intensity of the overtones with the overtone level.

4. Conclusions

The ν_s(X−H) stretching vibrations are characterized by high anharmonicity, which strongly depends on hydrogen-bonding interaction. On the other side, the anharmonicity is responsible for the interaction between high- and low-frequency modes, which is a source of wide, characteristic bands of ν_s(X−H···Y) vibrations. This information is not known for many systems, and theoretical calculations would be useful in that circumstance. These calculations, however, should be verified for the systems with very well documented anharmonicity. This is the case for phenol, where five transitions were determined in the gas phase at very low temperatures. These results were taken by us to verify the single-point calculations of the potential energy of phenol in the function of *r*(OH) distance. The harmonic calculations show that the ν_s(OH) mode consists exclusively of the O−H-stretching vibration. Conditions of the afore-mentioned experiment and calculations are very similar, and direct comparison seems to be appropriate. In calculations performed at the MP2/6-31G** level, it was shown that such an approach reproduces the ν_s(OH) transitions very well up to the fourth overtone.

Using the expansion of the dipole moment as a function of the *r*(OH) parameter, we were able to estimate the relative intensities of transitions and the influence of particular derivatives of dipole moments into the intensity of specific transitions, as well as the deuterium effect.

The frequencies of ν_s(OH) for the fundamentals and the first two overtones, for examined phenols, were determined from measurements in CCl_4 solution. It was found that these values correlate curvilinearly with pK_a. The curvature of the dependencies grows with the order of excitation. The results of the MP2/6-31G** calculations are in better agreement with experiment than the corresponding B3LYP values.

In the calculations of ν_s^{0n}(OH) frequencies, the possible conformational equilibria with respect to rotation of the −OH and $-CH_3$ groups were considered, and averaged values resulting from the Boltzmann distribution were applied in the correlations.

The influence of substituents on structural characteristics of phenols was presented as a function of pK_a. The equilibrium O−H distance increases upon substitution of electron-withdrawing groups, similarly to the C−O−H angle, while the C−O distance decreases. It was found that the calculations properly describe the trends in relative intensities of $0 \rightarrow 2$ and $0 \rightarrow 3$ transitions, with respect to the $0 \rightarrow 1$ transition. Similar slopes of dependency of the $0 \rightarrow 1$ transition intensity on pK_a in calculations and experiment were demonstrated. The observed tendencies in intensity changes were related to the changes of shape of the potential for the proton vibrations.

Acknowledgment. The measurements on the Bruker 66 spectrometer were done in Prof. Th. Zeegers-Huyskens's laboratory at the University of Leuven (Belgium). This work was supported by the Polish Committee for Scientific Research (grant KBN 7 T09A 008 21). Financial support from the Ministry of Education, Science, and Sports of Republic of Slovenia is acknowledged.

Supporting Information Available: Table 1S contains the experimental vibrational frequencies of fundamental, first, and second overtone transitions and the pK_a values of all 11 phenols. Tables 2S and 3S contain anharmonic vibrational frequencies of these 3 transitions calculated at MP2/6-31G** and B3LYP/6-31G** levels of theory, respectively. Table 4S contains the gas-phase acidities and anharmonic vibrational frequencies of fundamental transitions calculated at the MP2/6-31G** level of theory. This material is available free of charge via the Internet at http://pubs.acs.org.

References and Notes

(1) Sobczyk, L. *Ber. Bunsen-Ges. Phys. Chem.* **1998**, *102*, 3.

(2) Durocher, G.; Sandorfy, C. *J. Mol. Spectrosc.* **1967**, *22*, 347. (b) Conzi, M.; Huong, P. V. *Spectrochim. Acta, Part A* **1970**, *26*, 49.

(3) Czarnik-Matusewicz, B.; Chandra, A. K.; Nguyen, M. T.; Zeegers-Huyskens, Th. *J. Mol. Spectrosc.* **1999**, *195*, 308. (b) Rospenk, M.; Czarnik-Matusewicz, B.; Zeegers-Huyskens, T. *Spectrochim. Acta, Part A* **2001**, *57*, 185. (c) Zierkiewicz, W.; Michalska, D.; Zeegers-Huyskens, Th. *J. Phys. Chem. A* **2000**, *104*, 11685. (d) Michalska, D.; Rospenk, M.; Czarnik-Matusewicz, B.; Zeegers-Huyskens, Th. *J. Mol. Struct.* **2002**, *212*, 32. (e) Zierkiewicz, W.; Michalska, D.; Czarnik-Matusewicz, B.; Rospenk, M. *J. Phys. Chem. A* **2003**, *107*, 4547.

(4) Tishchenko, O.; Kryachko, E. S.; Nguyen, M. T. *Spectrochim. Acta, Part A* **2002**, *58*, 1951.

(5) Michalska, D.; Bieńko, D. C.; Abkowicz-Bieńko, A. J.; Latajka, Z. *J. Phys. Chem.* **1996**, *100*, 17786.

(6) Lampert, H.; Mikenda, W.; Karpfen, A. *J. Phys. Chem.* **1996**, *100*, 7418.

(7) Lampert, H.; Mikenda, W.; Karpfen, A. *J. Phys. Chem.* **1997**, *101*, 2254.
(8) Karesztury, G.; Billes, F.; Kubinyi, M.; Sundius, T. *J. Phys. Chem.* **1998**, *102*, 1371.
(9) Palomar, J.; De Paz, J. L. G.; Catalan, J. *Chem. Phys*. **1999**, *246*, 167.
(10) Yamada, Y.; Ebata, T.; Kayano, M.; Mikami, N. *J. Chem. Phys*. **2004**, *120*, 7400.
(11) Nguyen, M. T.; Kryachko, E. S.; Vanquickenborne, L. G. In *The Chemistry of Phenols*; Rappoport, Z., Ed.; The Chemistry of Functional Groups, Patai Series; Wiley: New York, 2003; Part 1, pp 1−198.
(12) Han, J.; Deming, R. L.; Tao, F.-M. *J. Phys. Chem. A* **2004**, *108*, 7736.
(13) Stare, J.; Mavri, J.; Ambrožič, G.; Hadži, D. *J. Mol. Struct*. **2000**, *500*, 429.
(14) Stare, J.; Jezierska, A.; Ambrožič, G.; Košir, I. J.; Kidrič, J.; Koll, A.; Mavri, J.; Hadži, D. *J. Am. Chem. Soc*. **2004**, *126*, 4437.
(15) Chaban, G. M.; Jung, J. O.; Gerber, R. B. *J. Chem. Phys*. **1999**, *111*, 182.
(16) del Bene, J. E.; Jordan, M. T. *Int. Rev. Phys. Chem*. **1999**, *18*, 119.
(17) Stare, J.; Mavri, J. *Comput. Phys. Commun.* **2002**, *143*, 222.
(18) Frisch, M. J.; Trucks, G. W.; Schlegel, H. B.; Scuseria, G. E.; Robb, M. A.; Cheeseman, J. R.; Zakrzewski, V. G.; Montgomery, J. A., Jr.; Stratmann, R. E.; Burant, J. C.; Dapprich, S.; Millam, J. M.; Daniels, A. D.; Kudin, K. N.; Strain, M. C.; Farkas, O.; Tomasi, J.; Barone, V.; Cossi, M.; Cammi, R.; Mennucci, B.; Pomelli, C.; Adamo, C.; Clifford, S.; Ochterski, J.; Petersson, G. A.; Ayala, P. Y.; Cui, Q.; Morokuma, K.; Malick, D. K.; Rabuck, A. D.; Raghavachari, K.; Foresman, J. B.; Cioslowski, J.; Ortiz, J. V.; Stefanov, B. B.; Liu, G.; Liashenko, A.; Piskorz, P.; Komaromi, I.; Gomperts, R.; Martin, R. L.; Fox, D. J.; Keith, T.; Al-Laham, M. A.; Peng, C. Y.; Nanayakkara, A.; Gonzalez, C.; Challacombe, M.; Gill, P. M. W.; Johnson, B. G.; Chen, W.; Wong, M. W.; Andres, J. L.; Head-Gordon, M.; Replogle, E. S.; Pople, J. A. *Gaussian 98*, revision A.11.1; Gaussian, Inc.: Pittsburgh, PA, 1998.
(19) Ischiuchi, S.; Shitomi, H.; Takazawa, K.; Fujii, M. *Chem. Phys. Lett*. **1998**, *283*, 243.
(20) Araújo, R. C. M. U.; da Silva, J. B. P.; de Barros Nato, B.; Ramos, M. N. *Chemom. Intell. Lab. Syst*. **2002**, *62*, 37.
(21) Herzberg, G. In *Molecular Spectra and Molecular Structure. V*ol. II. Infrared and Raman Spectra of Polyatomic Molecules; Van Nostrand: New York, 1956; Chapter 3.
(22) Wright, N. J.; Gerber, R. B. *J. Chem. Phys*. **2000**, *112*, 2598.
(23) Dkhissi, A.; Alkhani, M. E.; Bouteiller, Y. *THEOCHEM* **1997**, *416*, 1.
(24) Pedersen, T.; Larsen, N. W.; Nygaard, L. *J. Mol. Struct.* **1969**, *4*, 59.
(25) Di Paolo, T.; Bourdéron, C.; Sandorfy, C. *Can. J. Chem*. **1972**, *50*, 3161.
(26) Lehmann, K. K.; Smith, A. M. *J. Chem. Phys.* **1990**, *93*, 6140.
(27) Kjaergaard, H. G.; Daub, C. D.; Henry, B. R. *Mol. Phys*. **1997**, *90*, 201.
(28) Phillips, J. A.; Orlando, J. J.; Tyndall, G. S.; Vaida, V. *Chem. Phys. Lett*. **1998**, *296*, 377.
(29) Serjeant, E. P.; Dempsey, B. *Ionization Constants of Organic Acids in Solution*; IUPAC Chemical Data Series No. 23; Pergamon Press: Oxford, U.K., 1979.
(30) Lutz, B. T. G.; Langoor, M. H.; van der Maas, J. H. *Vib. Spectrosc*. **1998**, *18*, 111.
(31) Lutz, B. T. G.; van der Maas, J. H. *J. Mol. Struct*. **1997**, *436*−437, 213.
(32) Fujio, M.; McIver, R. T., Jr.; Taft, R. W. *J. Am. Chem. Soc*. **1981**, *103*, 4017.
(33) Majerz, I.; Malarski, Z.; Sobczyk, L. *Chem. Phys. Lett*. **1997**, *274*, 361.
(34) Yamamoto, N.; Shida, N.; Miyoshi, E. *Chem. Phys. Lett*. **2003**, *371*, 724.
(35) Koll, A.; Rospenk, M.; Jagodzińska, E.; Dziembowska, T. *J. Mol. Struct*. **2000**, *552*, 193.